Aminoalkyl Radicals: Direct Observation and Reactivity toward Oxygen, 2,2,6,6-Tetramethylpiperidine-*N*-oxyl, and Methyl Acrylate

J. Lalevée,* B. Graff, X. Allonas, and J. P. Fouassier

Department of Photochemistry, UMR 7525 CNRS, University of Haute Alsace, ENSCMu, 3 rue Alfred Werner, 68093 Mulhouse Cedex, France

Received: March 2, 2007; In Final Form: May 25, 2007

The reactivity of 11 aminoalkyl radicals toward different additives [oxygen, 2,2,6,6-tetramethylpiperidine-*N*-oxyl (TEMPO), and methyl acrylate (MA)] has been investigated through laser flash photolysis and quantum mechanical calculations. The transient absorption spectra of the radicals were recorded: good agreement was found with the spectra calculated by using quantum mechanical calculations. All the interaction rate constants were measured. A large range of values are obtained: $(0.04-3) \times 10^9$ M^{-1} s^{-1} for O_2, $(0.002-5) \times 10^8$ M^{-1} s^{-1} for TEMPO, and $(<0.004-2) \times 10^7$ M^{-1} s^{-1} for MA. Generation of the decarboxylated aminoalkyl radical derived from *N*-phenylglycine was unambiguously demonstrated. It was clearly found that both the addition to oxygen and the recombination with TEMPO were strongly governed by the reaction exothermicity. On the other hand, both polar and enthalpy factors have a large influence on the rate constants of the addition reaction to the acrylate unit, which were ranging over at least 4 orders of magnitude. This paper provides a set of new data to characterize the structure/reactivity relationships of aminoalkyl radicals.

Introduction

Aminoalkyl radicals are encountered in different fields of chemistry ranging from organic synthesis to polymer science.[1−2] In a general way, the search for radicals with low sensitivity to oxygen, having a given selectivity toward spin traps, or being able to add to double bonds can represent an interesting challenge. For example, these species are now recognized as the most powerful co-initiating systems for radical photopolymerization reactions.[2]

Despite the considerable interest in the reactivity of the radicals derived from amines, the rate constants of these reactions, as well as theoretical considerations, are rather scarce. On the other hand, few radicals have been directly observed and their reactivity is mainly based on indirect measurements. In this paper, 11 amines were considered (Scheme 1): some of them are efficient co-initiators, and the others are selected to get a large panel of different structures. The aim of this work is to investigate the reactivity of the corresponding aminoalkyl radicals toward three different reactants: oxygen, 2,2,6,6-tetramethylpiperidine-*N*-oxyl radical (TEMPO) as a spin trap, and methyl acrylate (MA) as a C−C double bond. The UV−visible absorption of these transient species was characterized by laser flash photolysis. To the best of our knowledge, no experimental data are available for R_2-R_{10} (Scheme 1). Thanks to their direct observation, their interaction with the additives can be probed. Quantum mechanical calculations allow us to calculate the absorption properties, reaction enthalpies, and transition states. Structure/reactivity relationships are discussed.

Experimental Section

The R_1-R_{10} aminoalkyl radicals presented in Scheme 1 are generated from triethylamine (TEA), methyldiethanolamine (MDEA), triisopropylamine (TIPA), 1,4-diazabicyclo[2.2.2]-octane (DABCO), triallylamine (TAA), tribenzylamine (TBA), dimethylaniline (DMA), dimethylaminobenzonitrile (DMABN), ethyl dimethylaminobenzoate (EDB), and *N*-phenylglycine (NPG), respectively. These amines (obtained from Aldrich) were used with the highest purity available except for TEA, MDEA, TIPA, DMA, and TBA (purified by distillation) and for DABCO (purified by sublimation). A polymeric derivative of EDB (poly-[oxy(methyl-1,2-ethanediyl)]-α-(4-dimethylamino)benzoyl-ω-butoxy, PDA, Speedcure PDA from Lambson Fine Chemicals) was also investigated: it leads to the R_{11} radical, which is structurally similar to R_9.

SCHEME 1

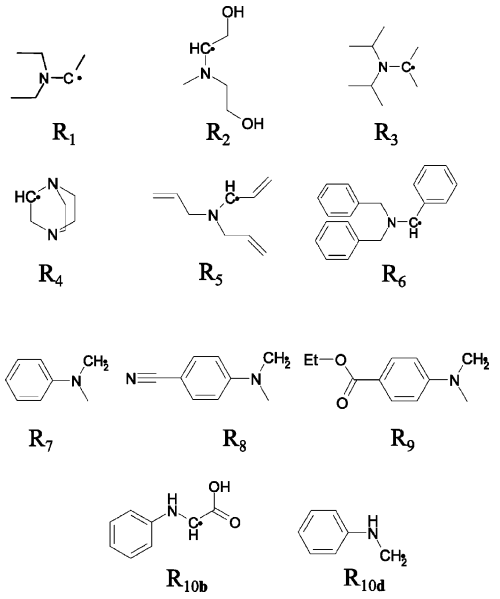

* Corresponding author: tel 33 (0)389336837; fax 33 (0)389336895; e-mail j.lalevee@uha.fr.

10.1021/jp071720w CCC: $37.00
Published on Web 07/03/2007

SCHEME 2

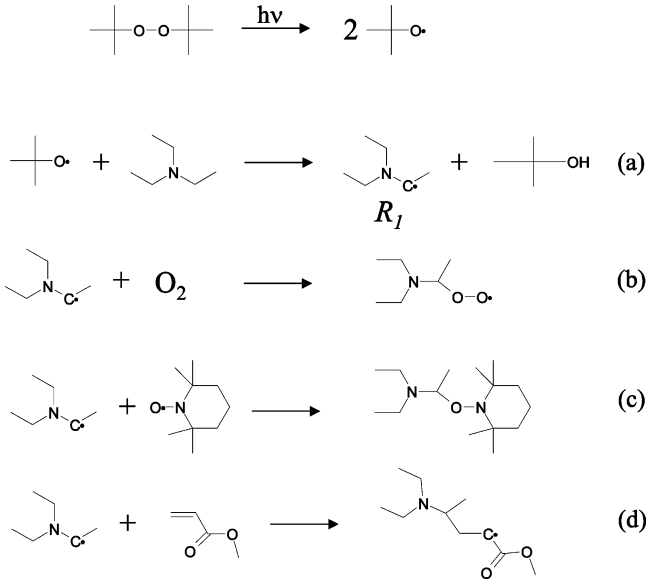

A well-known procedure was used for the production of the aminoalkyl radicals.[3] The first step consists of the generation of a *tert*-butoxyl radical through the photochemical decomposition of di-*tert*-butylperoxide. This radical does not absorb significantly above 300 nm. The second step corresponds to an α(C−H) hydrogen abstraction reaction between this radical and the amine.

Di-*tert*-butylperoxide and 2,2,6,6-tetramethylpiperidine-*N*-oxyl radical (TEMPO, Aldrich) have been received and used without further purification. For methyl acrylate (MA), the stabilizer (hydroquinone methyl ether) was removed by column purification (Aldrich AL-154).

The spectra and interaction rate constants characterizing the aminoalkyl radicals were determined by nanosecond laser flash photolysis (LFP): the setup, based on a pulsed Nd:Yag laser (Powerlite 9010, Continuum) operating at 10 Hz and delivering nanosecond pulses at 355 nm, has been already described in detail.[4] The time resolution is about 10 ns.

Molecular orbital calculations were carried out with the Gaussian 98 or 03 suite of programs.[5] The absorption spectra were calculated by time-dependent density functional theory (TDDFT) at TD/MPW1PW91/6-311++G** level on the basis of the frequency-checked geometries calculated at the UB3LYP/6-31G* level.

Structural and energetic factors governing the different reactions were determined by density functional theory (DFT), as previously described.[6−9] Calculations were carried out on fully optimized structures of the reactants, products, and transition states (TS) at the UB3LYP/6-31G* level. These geometries were frequency-checked, allowing us to calculate the zero-point energy (ZPE). The different reaction enthalpies (ΔH_r) for the processes investigated (a−d in Scheme 2) were calculated as the energy difference between the product and the reactants with the addition of the ZPE correction.

For the addition reaction (reaction d, Scheme 2), the amount of charge transfer (δ^{TS}) between the two moieties in the TS structure was calculated by use of the Mulliken charges. Single-point energy on optimized structures of both the reactants and the TS at the UB3LYP/6-311++G** level led to determination of the activation energy of the reaction (E_a). In the case of some reactions of aminoalkyl radicals with oxygen or TEMPO, both the relatively low barriers and the global spin multiplicity cause convergence instabilities that prevent a general calculation of the transition states.

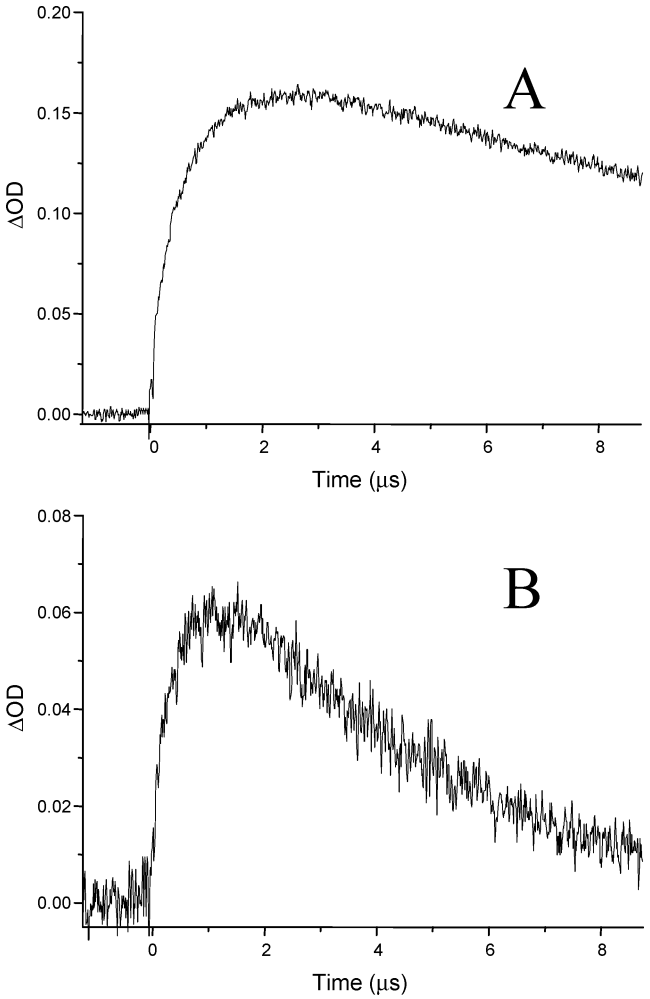

Figure 1. Kinetic traces for aminoalkyl radical formation and decay in di-*t*-butylperoxide/amine: (A) DMABN (0.012 M) and (B) EDB (0.006 M). Analysis wavelengths were 550 and 500 nm, respectively.

Results and Discussions

Generation of Aminoalkyl Radicals. The aminoalkyl radical produced according to Scheme 2 can be directly observed (Figure 1). The rising time gives a direct access to the hydrogen abstraction rate constants (k_H) of reaction (Table 1).

To characterize this reaction, the reaction exothermicity (ΔH_{ra}) was determined at the UB3LYP/6-31G* level (Table 1). The bond dissociation energies (BDE) evaluated for the parent amine—determined at the same level from an isodesmic reaction as realized previously in ref 4—are also given. As already observed,[4] the amine structure has little influence on the BDE values. The more pronounced differences are due to steric hindrance (DABCO) or delocalization (TAA, TBA) effects.

No clear correlation can be observed between k_H and the reaction abstraction exothermicity ΔH_{ra} (Table 1). Assuming that the activation energy is related to ΔH_r and therefore to the BDE, this lack of correlation is in agreement with previous studies on *t*-butoxyl/amine hydrogen abstraction reactions, which have underlined the huge effect of the activation entropy factor.[10] For R_1, R_2, R_5−R_9, and R_{11}, the formation rate constant k_H is higher or close to 10^8 M^{-1} s^{-1}. This rate constant being high for a hydrogen abstraction reaction[3] underlines the high reactivity of the corresponding amines toward this process.

TABLE 1: Rate Constants of the Interaction between *t*-Butoxyl Radical and Amine (Hydrogen Transfer Reaction)

amine	k_H (10^7 M^{-1} s^{-1})	BDE[a] (kJ/mol)	ΔH_{ra}[b] (kJ/mol)
TEA	11	381.6	−57.7
MDEA	20	387.1	−52.3
TIPA	0.3	384.2	−55.2
DABCO	0.8	416.8	−22.6
TAA	6	316.4	−122.2
TBA	6	336.0	−103.2
DMA	18	386.3	−53.3
DMABN	15	388.8	−50.4
EDB	23	388.4	−51.2
NPG	38	328.5	*c*
PDA	20	385.4	−51.9

[a] Determined from an isodesmic reaction by the same procedure as in ref 4 (UB3LYP/6-31G* level and ZPE-corrected). [b] Determined from optimized geometries of reactants and products at UB3LYP/6-31G*. [c] Not reported since a decarboxylation reaction takes place.

R_4 is characterized by both the lowest reaction exothermicity and the lowest k_H value. This effect was already reported and clearly ascribed to the entropy factor: the energy barrier was found to be similar for both R_1 and R_4, but only the activation entropy varies.[10]

The important steric hindrance in TIPA also leads to a lower k_H value.[4] As the reaction exothermicity is similar for R_1 and R_3, it is expected that the 35-fold decrease of k_H (compared to R_1) is attributable to an important activation entropy contribution.

For NPG, different sites for the hydrogen abstraction process can be considered. This special point will be discussed in the following section.

Spectra of Aminoalkyl Radicals. The spectra of the R_2-R_5 and R_8-R_{10} aminoalkyl radicals are depicted in Figure 2. The spectrum of R_1, centered at 340 nm, has been already reported in ref 11. For R_6 and R_7, very similar experimental absorption spectra have been reported in the literature (the other spectra are new).[3] The experimental absorption maxima as well as the predicted maxima evaluated from a time-dependent density functional theory approach (TDDFT) are gathered in Table 2. Despite the fact that the DFT method is now largely used for the prediction of UV−visible absorption properties of closed-shell systems,[12−14] only few data are available for radical structures. Although this method was recently found adapted for peroxyl and nitrogen-centered radicals,[15−17] almost no results have been published for carbon-centered radicals. Good agreement between the calculated and experimental absorption maxima can be noted (Table 2) despite slightly underestimated values for R_6, R_8, and R_9. The experimental and calculated data for R_1-R_5 and R_7 are within 10 nm. These results clearly support the contention that these methods can successfully describe the electronic transitions of various radicals.

Compared to R_1, a clear red shift is noted for R_4-R_9. The frontier molecular orbitals (MO) involved in these transitions (HDOMO−SOMO transitions were always noted) are found to be more delocalized in R_4-R_9 than in R_1, thereby reducing the energy gap and leading to a red-shifted absorption. In Figure 3, the main orbitals involved in the electronic transition of R_1 are compared to those characterizing R_4 and R_8. For R_1, the hyperconjugation between the carbon radical center and the nitrogen lone pair is mostly implied in the transition. For R_4, a through-bond interaction increases the delocalization of both molecular orbitals, resulting in a strongly shifted transition (from 340 to 400 nm). For R_8, this delocalization is enhanced due to the participation of the π system and a transition is observed at 550 nm. For PDA, the polymeric derivative radical R_{11}, an identical absorption spectrum as well as a similar reactivity to R_9 have been observed.

For NPG, different sites for the hydrogen abstraction process can be expected: on the nitrogen, the α(C−H) carbon, or the oxygen atom (Scheme 3) leading to radicals $R_{10a}-R_{10c}$, respectively. R_{10d} can be formed by an hydrogen abstraction process followed by a decarboxylation reaction as suspected in some previous works.[18] The experimental spectrum (Figure 2), which is very similar to that of R_7, should be ascribed to R_{10d}, as R_{10d} differs from R_7 only by the methyl substitution on the nitrogen atom. The calculated absorption spectra of the corresponding possible radicals, given in Table 2, are in favor of this assignment, although the presence of R_{10b} cannot be ruled out since the experimental transition is close to 400 nm. On the other hand, R_{10a} and R_{10c} can be excluded since the relative strength of the two reported UV transitions does not fit the observed spectrum; that is, the red-shifted transition exhibits a higher or equivalent intensity, in disagreement with the experimental findings.

This assignment is also in agreement with thermodynamic considerations. The respective N−H, C−H, and O−H BDEs being 358.6, 328.5, and 422.3 kJ/mol, it can be considered in a first step that the abstraction takes place predominantly on the carbon atom. However, the subsequent decarboxylation is calculated exothermic (36.1 kJ/mol), in agreement with the observation of R_{10d}. In the literature, a very fast decarboxylation reaction has been also suspected in previous works (Scheme 3).[18]

For MDEA, two sites of abstraction can also exist, leading to a secondary or a primary carbon-centered radical: both species may coexist in our experimental conditions, as no significant changes of the calculated absorption spectra were found (Table 2). The abstraction onto the oxygen atom was not considered since for the corresponding reaction $\Delta H_{ra} \approx 0$ kcal/mol.

Reactivity of Aminoalkyl Radicals toward Oxygen. The reaction is denoted b in Scheme 2. The kinetics observed in argon-saturated and air atmospheres for the decay of the aminoalkyl radical absorption as revealed by laser flash photolysis give direct access to the interaction rate constants (k_{O_2}) of these structures with oxygen (Table 3). The reaction exothermicities (ΔH_{rb}), calculated from the energy difference between the product (peroxyl radicals) and the reactants, are also gathered in this table. Among the structures studied, R_5 exhibits the lowest sensitivity to oxygen, with the other radicals having k_{O_2} values higher than 4×10^7 $M^{-1}s^{-1}$. For a large variety of other carbon-centered radicals, the reaction has been found to be diffusion-controlled with a nonselective value of about 3×10^9 M^{-1} s^{-1},[19] albeit different structures exhibiting a low reactivity have been also shown.[20−24]

The results of the MO calculations are worthwhile as exemplified by the clear correlation of ΔH_{rb} with k_{O_2} (Figure 4). For an exothermicity higher than 140 kJ/mol, the reaction is found close to the diffusion limit ($k_{O_2} = 3 \times 10^9$ M^{-1} s^{-1}). However, interestingly, when the exothermicity decreases, the rate constant falls, for example, for R_5, where $k_{O_2} = 4 \times 10^7$ M^{-1} s^{-1} and $\Delta H_{rb} = -58$ kJ/mol. The huge effect of ΔH_{rb} was previously suggested, albeit k_{O_2} was related only to the BDE of the parent amine.[20] The correlation obtained here (by use of ΔH_{rb}) is presumably more reliable since the BDE usually corresponds to an "indirect" parameter of the radical reactivity that characterizes its stability. Particularly some steric hindrance in peroxyl radical formation can be taken into account by the global enthalpy calculations. This result is of prime interest for

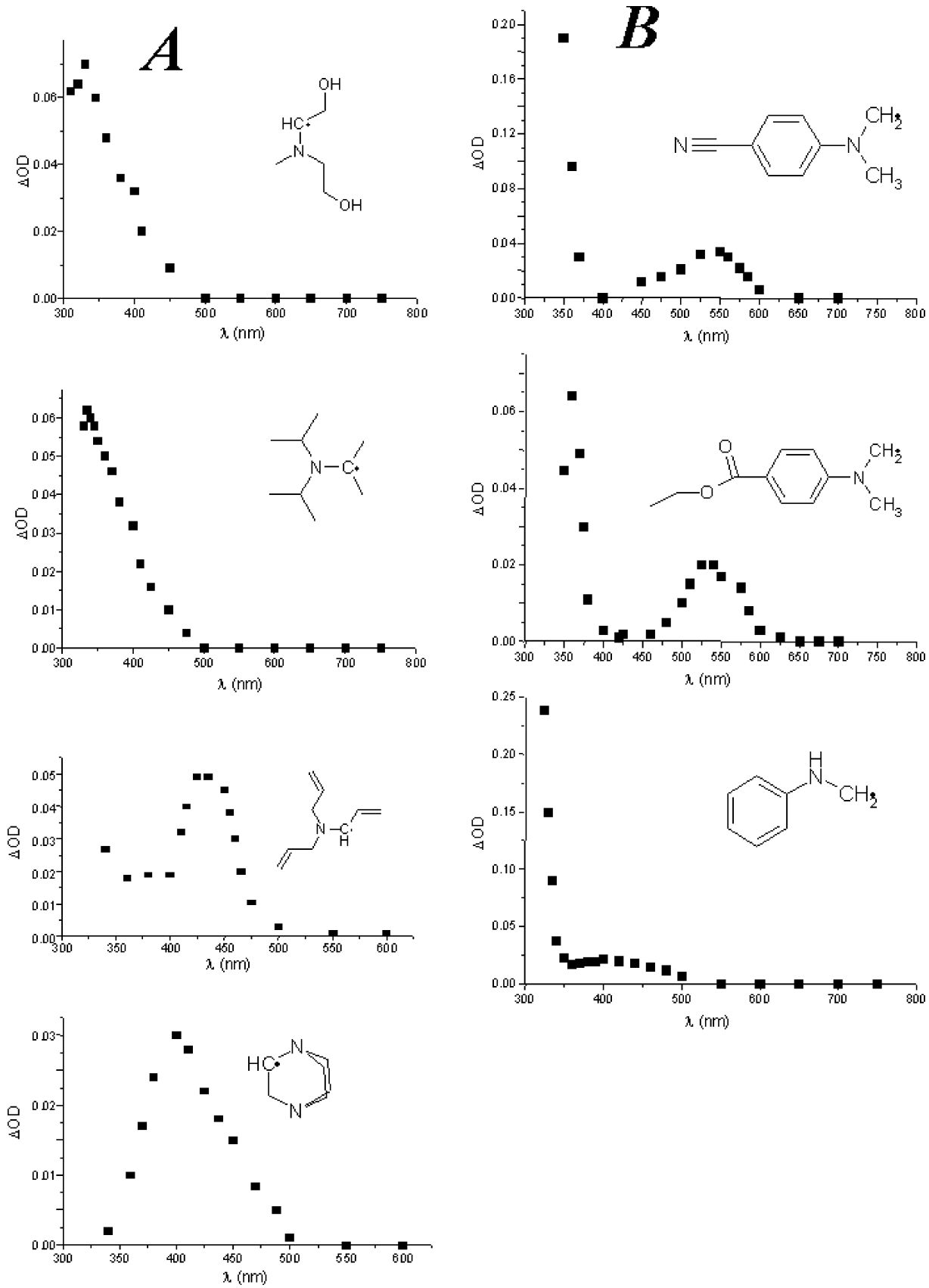

Figure 2. Transient absorption spectra (taken 500 ns after the laser flash) obtained in the di-*t*-butylperoxide/amine systems in acetonitrile. The quantity k_H[amine] is keep constant at 2×10^6 s^{-1}. (A) MDEA, TIPA, TAA, and DABCO; (B) DMABN, EDB, and NPG.

the understanding of reactive oxygen species (ROS) formation or the design of oxygen-insensitive radicals, allowing the finding of new, more efficient radical structures in polymerization reactions.

Reactivity of Aminoalkyl Radicals toward TEMPO. The reactivity of the R_1-R_{11} radicals toward TEMPO is also particularly worthwhile. An example of the Stern−Volmer analysis is depicted in Figure 5. The interaction rate constants

TABLE 2: Comparison of Calculated and Experimental Absorption Maxima of Aminoalkyl Radicals

radical	λ_{max} (exp),[a] nm	λ_{max} (calc),[b] nm
R_1	340	356.2 [0.047]
R_2	330	322.9 [0.0345]; 321.1 [0.039][c]
R_3	335	338.4 [0.0114]
R_4	400	407.4 [0.011]
R_5	430	432.2 [0.01]
R_6	490; <350	427.5 [0.006]; 381.3 [0.01]; 364 [0.015]
R_7	410; <350	415.3 [0.005]; 394.7 [0.011]; 377.3 [0.0196]; 325.9 [0.056]; 319.2 [0.147]
R_8	540; <350	460.5 [0.051]; 350.6 [0.083]; 348.5 [0.199]
R_9	530; 360	467.9 [0.076]; 360.7 [0.024]; 351.6 [0.259]
R_{10a}	400; <320	369.1 [0.031]; 297 [0.031]
R_{10b}		406.9 [0.0375]; 314.5 [0.369]
R_{10c}		387.9 [0.078] 300.8 [0.031]
R_{10d}		412.9 [0.0043]; 307.4 [0.176]
R_{11}	530; 360	470.9 [0.086]; 365.2 [0.028]; 356.2 [0.278]

[a] Experimental data extracted from Figure 2. [b] At TD/MPW1PW91/6-311++G** on the geometries optimized at UB3LYP/6-31G* level. Oscillator strength is given in brackets. [c] Abstraction of hydrogen on the methyl group, leading to a primary carbon-centered radical.

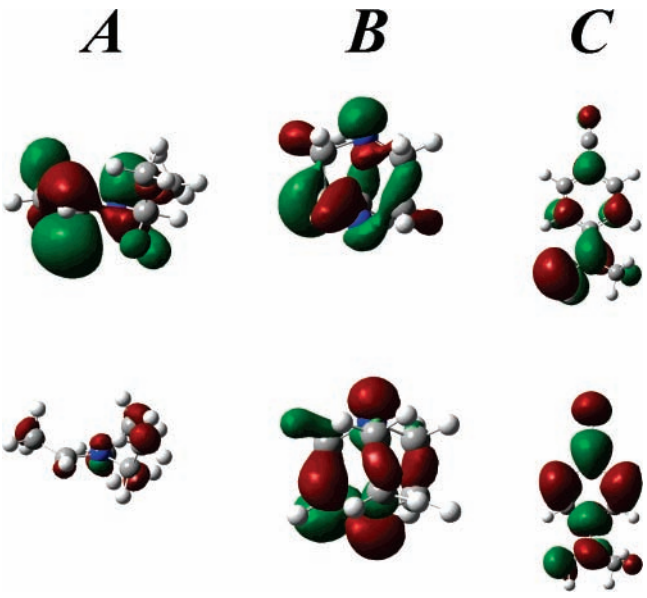

Figure 3. Orbitals involved in the electronic transition for (A) R_1, (B) R_4, and (C) R_8. The first row corresponds to the starting orbital for the electronic transition.

SCHEME 3

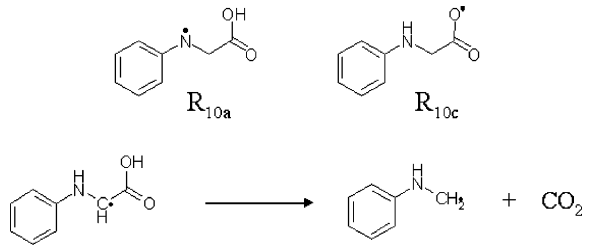

(k_{TEMPO}) are gathered in Table 4 together with the reaction exothermicities (ΔH_{rc}) obtained at UB3LYP/6-31G* level. The change of log (k_{TEMPO}) vs ΔH_{rc} is given in Figure 4B. For radicals characterized by an exothermicity higher than 80 kJ/mol, a high reactivity is observed as supported by the interaction rate constants exhibiting limit values close to 3×10^8 $M^{-1}s^{-1}$. This plateau is typical of efficient reactions between carbon-centered radicals and TEMPO. It is also very similar to those recently found for the acrylate radicals.[11,25] However, even for highly exothermic reactions, the steric hindrance directly affects the rate constants, that is, lower k_{TEMPO} than expected from the plateau value are obtained (ranging between 3×10^7 and 3×10^8 M^{-1} s^{-1}). This contention is well exemplified by triisopropylamine (with bulky substituents),[4] which is characterized by the lowest value in this exothermicity domain.

TABLE 3: Rate Constants of the Interaction between Aminoalkyl Radicals and Oxygen

radical	k_{O_2} (10^9 M^{-1} s^{-1})	ΔH_{rb}[a] (kJ/mol)
R_1	2.9	−135.9
R_2	1.5	−119.9
R_3	0.9	−133.2
R_4	3.0	−148.8
R_5	0.04	−58.8
R_6	0.45	−91.8
R_7	1.5	−119.7
R_8	0.6	−114.6
R_9	0.5	−115.7
R_{10d}	0.9	−123.6
R_{11}	0.8	−116.4

[a] Determined from optimized geometries of reactants and products at UB3LYP/6-31G*.

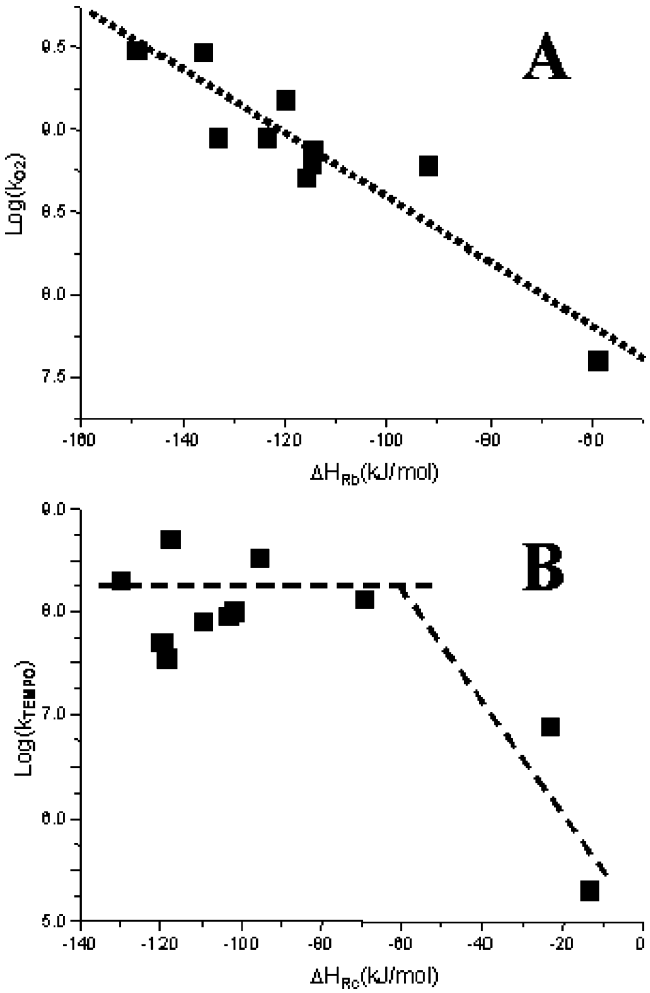

Figure 4. (A) Plot of log (k_{O_2}) vs ΔH_{rb} (the correlation line obtained by least-square fit is shown). (B) Plot of log (k_{TEMPO}) vs ΔH_{rc} (the dashed lines are not correlation lines).

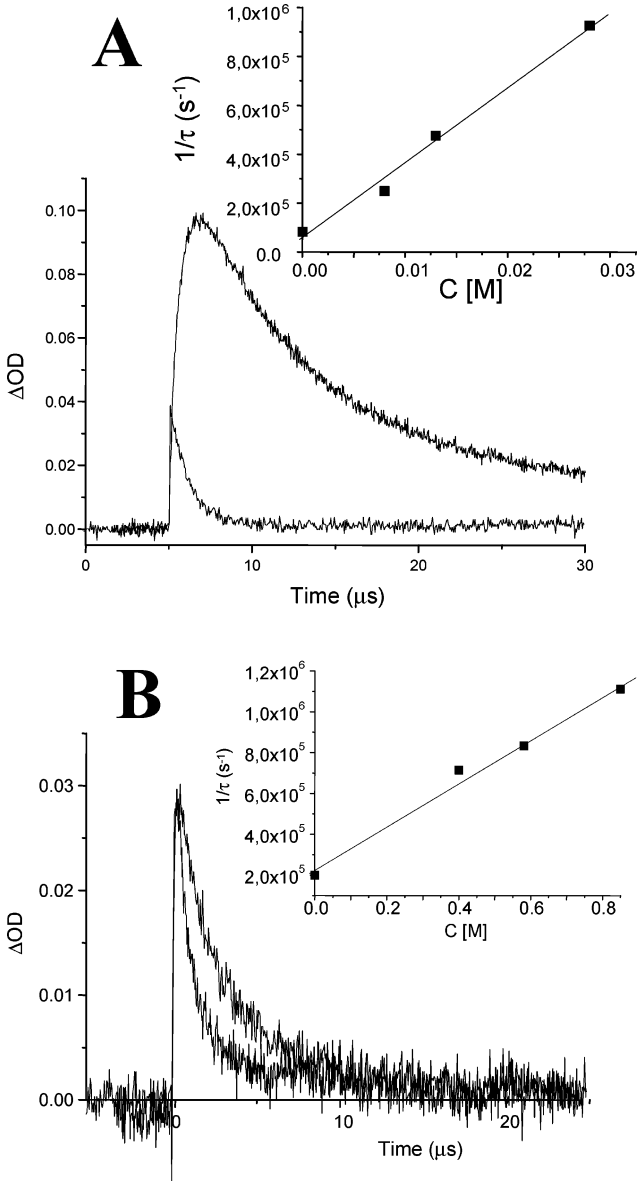

Figure 5. (A) Quenching of R_8 by TEMPO: kinetic traces at 350 nm for 0 and 0.027 M TEMPO. (B) Quenching of R_7 by MA: kinetic traces at 360 nm for 0 and 0.58 M MA. Insets: corresponding Stern−Volmer plots.

TABLE 4: Rate Constants of the Interaction between Aminoalkyl Radicals and TEMPO

radical	k_{TEMPO} (10^8 M^{-1} s^{-1})	ΔH_{rc}[a] (kJ/mol)
R_1	3.3	−95.4
R_2	5.0	−117.6
R_3	1.3	−69.1
R_4	2.0	−129.6
R_5	0.002	−13.3
R_6	0.075	−23.4
R_7	0.5	−119.6
R_8	0.35	−118.4
R_9	1.0	−101.8
R_{10d}	0.8	−109.4
R_{11}	0.8	−102.5

[a] Determined from optimized geometries of reactants and products at UB3LYP/6-31G*.

The rate constants markedly fall with decreasing exothermicity down to 40 kJ/mol. Interestingly, Figure 6 shows that k_{TEMPO} decreases with k_{O_2}. The dependence of the rate constants of the aminoalkyl radicals with oxygen and TEMPO on ΔH_r is

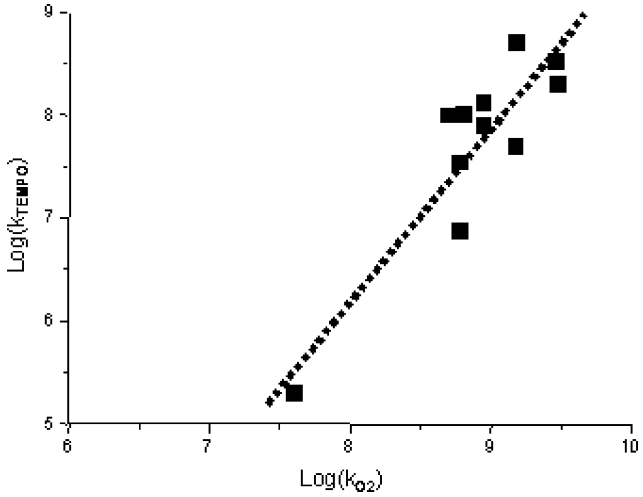

Figure 6. Plot of log (k_{TEMPO}) vs log (k_{O_2}).

in good agreement with recent statements suspecting that both reactions were strongly related and governed by the BDE of the parent hydrogenated compound.[20]

Reactivity of Aminoalkyl Radicals toward a Double Bond. The interaction rate constants (k_{MA}) between the R_1-R_{11} radicals and methyl acrylate (reaction d in Scheme 2) are gathered in Table 5 and an example of the Stern−Volmer analysis is given in Figure 5. R_1 is very reactive (k_{MA} are 20−100 times higher than for R_3, R_4, or R_7-R_{10}). Interestingly, R_5 and R_6 are unreactive (k_{MA} are lower than 4×10^4 M^{-1} s^{-1}). Interestingly, it was already noted above that these radicals are also less reactive than the others toward O_2 and TEMPO. The reaction exothermicities (ΔH_{rd}), determined from the energies of the reactants and products as previously done for reactions a−c, are gathered in Table 5. The complete procedure for the calculations of the transition states (TS) properties—presented in detail in refs 6−9—allows for determination of the energy barrier. The validity of these calculations is reflected (Figure 7) in the excellent linear relationship observed between log (k_{MA}) and the energy barrier (as expected from the classical Arrhenius equation).

The preexponential factor in the Arrhenius equation (A) is given by the activated complex theory:[26,27]

$$A = \chi \frac{k_B T}{h} (R'T)^{-\Delta n^*} \exp(1 - \Delta n^*) \exp\left(\frac{\Delta S^*}{R}\right) \qquad (1)$$

where ΔS^* and Δn^* are the entropy and number of particle changes in going to the TS structure, respectively. k_B is the Boltzmann constant, R is the ideal gas constant, T is the temperature in absolute units, h is the Planck constant, and χ is the transmission coefficient (taken here equal to 1). The harmonic oscillator approximation was adopted for the ΔS^* calculations (Table 5), allowing us to determine A by eq 1. This treatment was assumed in the literature[26] to be accurate enough to describe the addition of carbon-centered radicals into double bonds. The calculated addition rate constants, gathered in Table 5, are found to be 1 order of magnitude lower than the experimental ones. Since the calculations of the activation energy can be considered as accurate enough for aminoalkyl radicals,[6−9] the main error can be ascribed to the preexponential factor calculation. This could result from the combination of two different factors: (i) the influence of the solvent, which is not included and could affect the preexponential factor,[28] and (ii) the description of the low-frequency torsionnal modes as vibrations, which is used for the calculations of the rate constants

TABLE 5: Rate Constants of the Addition of Aminoalkyl Radicals to Methyl Acrylate

radical	k_{MA}[a] (10^7 M^{-1} s^{-1})	ΔH_{rd}[b] (kJ/mol)	ΔS^* (J mol^{-1} K^{-1})	δ^{TS}	energy barrier[c] (kJ/mol)	k_{MA} (calc)[d] (M^{-1} s^{-1})
R_1	2.0×10^7	−71.3	−167.2	0.199	2.0	9.7×10^5
R_2	9.0×10^6	−91.1	−151.1	0.175	7.8	6.1×10^5[e]
R_3	6.0×10^5	−45.7	−202.1	0.246	3.8	6.6×10^3
R_4	9.0×10^5	−118.6	−167.8	0.08	8.95	5.2×10^4
R_5	$<4.0 \times 10^4$	−21.5	−170.3	0.185	49.7	3×10^{-3}
R_6	$<4.0 \times 10^4$	−42.2	−192.5	0.167	33.7	0.1
R_7	9.7×10^5	−90.5	−164.5	0.137	9.9	5.05×10^4
R_8	3.0×10^5	−91.3	−165.7	0.106	14.2	7.9×10^3
R_9	5.0×10^5	−91.0	−166.1	0.118	12.5	1.5×10^4
R_{10a}		−39.4	−171.2	0.014	49.6	0.003
R_{10b}		−22.4	−184.5	0.081	38.6	0.05
R_{10c}		−60.5	−179.5	0.015	16.2	680
R_{10d}	6.5×10^5	−94.6	−150.7	0.12	13.1	7.8×10^4
R_{11}	6.2×10^5	−92.1	*f*	*f*	*f*	*f*

[a] Experimental interaction rate constants. [b] Determined from optimized geometries of reactants and products at UB3LYP/6-31G*. [c] From single point at UB3LYP/6-311++G** on the geometries (reactant and TS structure) determined at UB3LYP/6-31G* level and ZPE-corrected at UB3LYP/6-31G* level. [d] Calculated values form eq 1 see text. [e] For the primary carbon-centered radicals of MDEA, a calculated value of 7.2×10^5 M^{-1} s^{-1} was obtained. [f] The transition state for R_{11} was not calculated, this radical being too large for the computation.

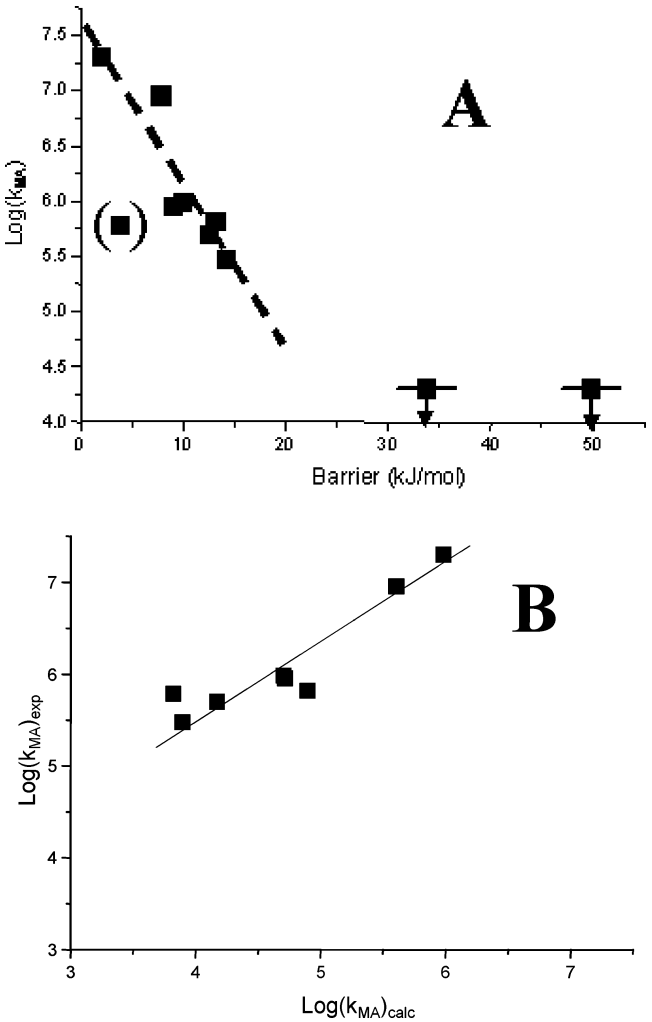

Figure 7. (A) Plot of log (k_{MA}) vs the calculated barrier. (B) Plot of log $(k_{MA})_{exp}$ vs log $(k_{MA})_{calc}$.

from the activated complex theory. The latter effect was recently given as evidence for the addition of a carbon-centered radical into a C═S bond.[29−30] However, despite the harmonic oscillator approximation used for the evaluation of *A*, an excellent correlation (Figure 7) between the calculated and experimental values is observed. R_5 and R_6 are not included in the latter correlation since only limiting values for k_{MA} are available. The values from the calculations (Table 5) are expected to be lower than 4×10^4 M^{-1} s^{-1}, in full agreement with the experimental ones. For R_3 and R_6 hindered radicals, ΔS^* is lower by about 33.5 and 25.1 J mol^{-1} K^{-1}, respectively, than the other radicals: the TS structures are more crowded leading to a more negative activation entropy. This results in a lower preexponential factor (*A*). For R_3, despite a low barrier, k_{MA} is 30 times lower than for R_1: this is also ascribed to its lower *A* value (this is the reason why R_3 is given in parentheses in Figure 7A).

For the radical derived from NPG, quite good reactivity is observed with $k_{MA} = 6.5 \times 10^5$ M^{-1} s^{-1}. Among the different structures considered in Scheme 3, only R_{10d} appears plausible, the calculated value being 7.8×10^4 M^{-1} s^{-1} (Table 5). This unambiguously demonstrates that a fast decarboxylation of the radical formed after the hydrogen abstraction process occurs: the transient spectrum observed in the case of NPG can be confidently assigned to R_{10d}. This has a significant consequence in photopolymerization reactions where a photoinitiator (e.g., a benzophenone derivative) absorbs the irradiation light and, after intersystem crossing, is promoted into its excited triplet state, which further abstracts an hydrogen atom from the amine. In fact, it is well-known that NPG exhibits a higher reactivity than a classical amine.[18c] From our results, this behavior cannot be ascribed to a higher reactivity of the generated radical in the initiation step. Indeed, k_{MA} for R_{10d} is significantly lower than for R_2 or equivalent to that for R_9, which correspond to two widely used industrial co-initiators. This particular behavior of NPG can be now likely ascribed to the fast proton transfer and/or the decarboxylation reaction, which avoids the back electron-transfer reaction in the ketone triplet state/NPG system [as shown in Table 1, the α(C−H) BDE of NPG is 328.5 kJ/mol compared to ∼380 kJ/mol for classical amines]. The behavior of NPG in photopolymerization processes, which is beyond the scope of this study, will be investigated in detail in forthcoming papers.

Another valuable result can also be obtained from the R_9/R_{11} reactivity comparison; that is, the polymeric structure (PDA) exhibits the same reactivity as EDB. This result unambiguously demonstrates the weak influence of the polymer chain length on the addition rate constant.

Despite that k_{MA} was roughly related to ΔH_{rd} (Table 5), some deviations are observed. For example, R_1 appears as the most efficient radical despite a reaction exothermicity lower than R_4 or R_7−R_9. As evidenced previously, the radical addition reaction

to an acrylate unit exhibits a strong interplay between enthalpy and polar contributions.[6−9] This polar effect, ascribed to the participation of the charge-transfer configurations R^+/M^- or R^-/M^+ to the transition-state (TS) structure, can be evaluated from the amount of charge transfer (δ^{TS}) from the radical to MA in TS by using the Mulliken charges.[28] It can be observed in Table 5 that R_1 is characterized by a strong polar effect, higher than for R_4 or R_7-R_9. This polar effect is also high for R_5 and R_6, although the enthalpy term (ΔH_{rd}) is too weak for expecting a high interaction rate constant. These results well explain why the complete set of data does not reveal any stringent correlation between k_{MA} and k_{O_2} or k_{TEMPO}. This lack of correlation is due to the fact that both polar and enthalpy effects govern the radical/acrylate interaction,[6−9] whereas enthalpy effects are probably mostly controlling k_{O_2} and k_{TEMPO}.

Conclusion

MO calculations have underlined the crucial role of the reaction exothermicity to explain how the reactivity of the aminoalkyl radical is influenced by its chemical structure. The reactivity toward oxygen is reduced when $\Delta H_r < 120-130$ kJ/mol. In the case of TEMPO, this term lies between 40 and 100 kJ/mol. These results will be likely useful for the design of radical structures in order to get an insight on their reactivity toward these strong radical inhibitors. In the particular addition reaction of an aminoalkyl radical to an acrylate unit, the polar and enthalpy factors have a huge effect as revealed by the interaction rate constants ranging over at least 4 orders of magnitude. This work will be extended to other carbon- or sulfur-centered structures in forthcoming studies.

Acknowledgment. We thank CINES (Centre Informatique National de l'Enseignement Supérieur) for the generous allocation of time on the IBM SPsupercomputer.

References and Notes

(1) Bertrand, S.; Hoffmann, N.; Humbel, S.; Pete, J. P. *J. Org. Chem.* **2000**, *65*, 8690.

(2) (a) Fouassier, J. P. *Photoinitiation Photopolymerization and Photocuring*; Hanser Publishers: Munich and New York, 1995. (b) *Photochemistry and UV curing: New trends*; Fouassier, J. P., Ed.; Research Signpost: Trivandrum, India, 2006.

(3) (a) Scaiano, J. C. *J. Phys. Chem.* **1981**, *85*, 2851. (b) Griller, D.; Howard, J. A.; Marriott, P. R.; Scaiano, J. C. *J. Am. Chem. Soc.* **1981**, *103*, 619.

(4) Lalevée, J.; Allonas, X.; Fouassier, J. P. *J. Am. Chem. Soc.* **2002**, *124*, 9613.

(5) Frisch, M. J.; Trucks, G. W.; Schlegel, H. B.; Scuseria, G. E.; Robb, M. A.; Cheeseman, J. R.; Montgomery, J. A., Jr.; Vreven, T.; Kudin, K. N.; Burant, J. C.; Millam, J. M.; Iyengar, S. S.; Tomasi, J.; Barone, V.; Mennucci, B.; Cossi, M.; Scalmani, G.; Rega, N.; Petersson, G. A.; Nakatsuji, H.; Hada, M.; Ehara, M.; Toyota, K.; Fukuda, R.; Hasegawa, J.; Ishida, M.; Nakajima, T.; Honda, Y.; Kitao, O.; Nakai, H.; Klene, M.; Li, X.; Knox, J. E.; Hratchian, H. P.; Cross, J. B.; Bakken, V.; Adamo, C.; Jaramillo, J.; Gomperts, R.; Stratmann, R. E.; Yazyev, O.; Austin, A. J.; Cammi, R.; Pomelli, C.; Ochterski, J. W.; Ayala, P. Y.; Morokuma, K.; Voth, G. A.; Salvador, P.; Dannenberg, J. J.; Zakrzewski, V. G.; Dapprich, S.; Daniels, A. D.; Strain, M. C.; Farkas, O.; Malick, D. K.; Rabuck, A. D.; Raghavachari, K.; Foresman, J. B.; Ortiz, J. V.; Cui, Q.; Baboul, A. G.; Clifford, S.; Cioslowski, J.; Stefanov, B. B.; Liu, G.; Liashenko, A.; Piskorz, P.; Komaromi, I.; Martin, R. L.; Fox, D. J.; Keith, T.; Al-Laham, M. A.; Peng, C. Y.; Nanayakkara, A.; Challacombe, M.; Gill, P. M. W.; Johnson, B.; Chen, W.; Wong, M. W.; Gonzalez, C.; Pople, J. A. *Gaussian 98*, revision A.11; Gaussian, Inc.: Pittsburgh, PA, 2001.

(6) Lalevée, J.; Allonas, X.; Fouassier, J. P. *J. Am. Chem. Soc.* **2003**, *125*, 9377.

(7) Lalevée, J.; Allonas, X.; Fouassier, J. P. *J. Phys. Chem. A.* **2004**, *108*, 4326.

(8) Lalevée, J.; Allonas, X.; Fouassier, J. P. *J. Org. Chem.* **2005**, *70*, 814.

(9) Lalevée, J.; Allonas, X.; Fouassier, J. P. *Macromolecules* **2005**, *38*, 4521.

(10) (a) Finn, M.; Friedline, R.; Suleman, N.; Wohl, C. J.; Tanko, J. M. *J. Am. Chem. Soc.* **2004**, *126*, 7578. (b) Tanko, J. M.; Friedline, R.; Suleman, N.; Castagnoli, N. *J. Am. Chem. Soc.* **2001**, *123*, 5808.

(11) Lalevée, J.; Allonas, X.; Fouassier, J. P. *Chem. Phys. Lett.* **2005**, *415*, 287.

(12) Jacquemin, D.; Preat, J.; Wathelet, V.; Perpète, E. A. *THEOCHEM* **2005**, *731*, 67.

(13) Tozer, D. J.; Amos, R. D.; Handy, N. C.; Roos, B. O.; Serrano-Andrès, L. *Mol. Phys.* **1999**, *97*, 859.

(14) Han, W. G.; Liu, T.; Hima, F.; Toutchkine, A.; Bashford, D.; Hahn, K. N.; Noodleman, L. *ChemPhysChem* **2003**, *4*, 1084.

(15) Weisman, J. L.; Head-Gordon, M. *J. Am. Chem. Soc.* **2001**, *123*, 11686.

(16) Hirata, S.; Head-Gordon, M. *Chem. Phys. Lett.* **1999**, *302*, 375.

(17) DiLabio, G. A.; Litwinienko, G.; Lin, S.; Pratt, D. A.; Ingold, K. U. *J. Phys. Chem. A* **2002**, *106*, 11719.

(18) (a) Totah, R. A.; Hanzlik, R. P. *Biochemistry* **2004**, *43*, 7907. (b) Rajesh, C. S.; Thanulingam, T. L.; Das, S. *Tetrahedron* **1997**, *53*, 16817. (c) Ullrich, G.; Burtscher, P.; Salz, U.; Moszner, N.; Liska, R. *J. Polym. Sci., Part A: Polym. Chem.* **2006**, *44*, 115.

(19) Maillard, B.; Ingold, K. U.; Scaiano, J. C. *J. Am. Chem. Soc.* **1983**, *105*, 5095.

(20) Font-Sanchis, E.; Aliaga, C.; Bejan, E. V.; Cornejo, R.; Scaiano, J. C. *J. Org. Chem.* **2003**, *68*, 3199.

(21) Font-Sanchis, E.; Aliaga, C.; Focsaneanu, K. S.; Scaiano, J. C. *Chem. Commun.* **2002**, 1576.

(22) Scaiano, J. C.; Martin, A.; Yap, G. P. A.; Ingold, K. U. *Org. Lett.* **2000**, *2*, 899.

(23) Frenette, M.; Aliaga, C.; Font-Sanchis, E.; Scaiano, J. C. *Org. Lett.* **2004**, *6*, 2579.

(24) (a) Bejan, E. V.; Font-Sanchis, E.; Scaiano, J. C. *Org. Lett.* **2001**, *3*, 4059. (b) Font-Sanchis, E.; Aliaga, C.; Cornejo, R.; Scaiano, J. C. *Org. Lett.* **2003**, *5*, 1515.

(25) Sobeck, J.; Martschke, R.; Fischer, H. *J. Am. Chem. Soc.* **2001**, *123*, 2849.

(26) Arnaud, R.; Subra, R.; Barone, V.; Lelj, F.; Olivella, S.; Solé, A.; Russo, N. *J. Chem. Soc., Perkin Trans. 2* **1986**, 1517.

(27) Pacey, P. D. *J. Chem. Educ.* **1981**, *58*, 612.

(28) Fischer, H.; Radom, L. *Angew. Chem., Int. Ed.* **2001**, *40*, 1340.

(29) Coote, M. L. *Macromolecules* **2004**, *37*, 5023.

(30) Henry, D. J.; Coote, M. L.; Gomez-Balderas, R.; Radom, L. *J. Am. Chem. Soc.* **2004**, *126*, 1732.